Brucella abortus induces a Warburg shift in host metabolism that enhances intracellular replication of the pathogen

Daniel M. Czyż[a,b], Jonathan Willett[a,b], Sean Crosson[a,b,c#]

Howard Taylor Ricketts Laboratory, University of Chicago, Argonne National Laboratory, Lemont, Illinois, USA[a]; Department of Biochemistry and Molecular Biology, University of Chicago, Chicago, Illinois, USA[b]; Department of Microbiology, University of Chicago, Chicago, Illinois, USA[c]

Running title: *Brucella abortus* infection and host cell metabolism

[#]Address correspondence to Sean Crosson, scrosson@uchicago.edu

KEYWORDS: Metabolism, Warburg effect, lactate, Brucella, therapeutics

ABSTRACT

Intracellular bacterial pathogens exploit host cell resources to replicate and survive inside the host. Targeting these host systems is one promising approach to developing novel antimicrobials for intracellular infections. We show that human macrophage-like cells infected with *Brucella abortus* undergo a metabolic shift characterized by attenuated tricarboxylic acid cycle metabolism, altered mitochondrial morphology and increased lactate production. This shift to an aerobic glycolytic state resembles the Warburg effect, a change in energy production that is well-described in cancer cells, and also occurs in activated inflammatory cells. *B. abortus* efficiently uses lactic acid as a carbon and energy source and requires the ability to metabolize lactate for normal replication in human macrophage-like cells. We further demonstrate that chemical inhibitors of host glycolysis and lactate production do not affect *in vitro* growth of *B. abortus* in axenic culture, but decrease its replication in the intracellular niche. Our data support a model in which infection shifts host metabolism to a Warburg-like state, and *B. abortus* uses this change in metabolism to promote intracellular replication. Pharmacological perturbation of these features of host cell metabolism may be a useful strategy to inhibit infection by intracellular pathogens.

IMPORTANCE

Brucella spp. are intracellular pathogens that cause disease in a range of mammals, including livestock. Transmission from livestock to humans is common and can lead to chronic human disease. Human macrophage-like cells infected with *Brucella abortus* undergo a Warburg-like metabolic shift to an aerobic glycolytic state that produces lactic acid, which *B. abortus* can use as a carbon and energy source to promote its growth.

39 We provide evidence that the pathogen exploits this change in host metabolism to
40 replicate in the intracellular niche. Drugs that target this feature of host cell metabolism
41 inhibit intracellular replication of *B. abortus* and may be broadly useful therapeutics for
42 intracellular infections.

43 **INTRODUCTION**

44 Macrophages can be activated by pathogen-associated pro-inflammatory
45 molecules such as lipopolysaccharide (LPS). Classically activated (i.e. M1)
46 macrophages undergo a major metabolic shift in which the tricarboxylic acid (TCA)
47 cycle is downregulated, and energy production transitions from oxidative
48 phosphorylation to the less efficient process of aerobic glycolysis (1, 2). This change in
49 metabolism, known as the Warburg effect (3), is a well-described metabolic feature of
50 cancer cells (4). Increased glucose consumption through glycolysis is thought to
51 increase adenosine triphosphate (ATP) levels; a corresponding increase in pentose
52 phosphate pathway activity generates nicotinamide adenine dinucleotide phosphate
53 (NADPH), which is subsequently used by NADPH oxidases to generate reactive oxygen
54 species (ROS) (5). This metabolic shift is important in enabling cells to launch general
55 antimicrobial defense mechanisms by increasing concentrations of ROS and reactive
56 nitrogen intermediates (6).

57 The intracellular pathogen *Brucella abortus* invades host cells and is trafficked to
58 a compartment known as the Brucella containing vacuole, where it replicates. To
59 successfully find its way to this niche, *B. abortus* must avoid numerous chemical insults
60 by the host cell and adapt to the nutrient resources available within the host. The

61 mechanisms by which *B. abortus* evades host defenses and takes advantage of host
62 metabolic responses remain understudied. *B. abortus* induces a Warburg-like effect in
63 mammalian host cells. We demonstrate that this metabolic shift is advantageous for *B.*
64 *abortus* replication, and that chemical inhibition of Warburg metabolism in macrophage-
65 like cells attenuates intracellular replication of *B. abortus*. Thus, *B. abortus* exploits an
66 innate immune metabolic response to support infection.

67

68 **RESULTS**

69 ***Brucella abortus* infection of human macrophage-like cells disrupts mitochondrial**
70 **function and morphology**

71 To characterize the effect of intracellular colonization by *B. abortus* on human
72 cell metabolism, we employed mammalian cell phenotype microarrays (PM) to measure
73 respiration in terminally differentiated, metabolically active THP-1 cells. These cells
74 were cultivated in minimal essential medium in the presence of central metabolic
75 substrates specifically selected to measure mitochondrial function. Three of the
76 substrates, α-ketoglutaric acid, β-hydroxybutyric acid, and pyruvic acid are metabolized
77 in mitochondria. We assessed the respiration of the human cells solely utilizing the
78 provided substrate as a primary energy source by colorimetrically measuring reduction
79 of a redox indicator dye. This assay allows us to assess the cells' ability to metabolize
80 substrates across different molecular pathways, and thus provides a measurement of
81 metabolic pathway activity upon infection (Figure 1A). We infected the cells with *B.*
82 *abortus* at increasing multiplicities of infection (MOI). To eliminate the possibility that

83 changes in the metabolic activity of human cells are caused by *Brucella*-induced cell
84 death, we removed medium containing mitochondrial substrates and replaced it with a
85 regular growth medium containing glucose, followed by assessment of cell viability
86 using the MTT (3-(4,5-dimethylthiazol-2-yl)-2,5-diphenyltetrazolium bromide) assay. The
87 number of viable cells remained the same at different *Brucella* MOI (Figure 1B). Naïve
88 cells utilized all of the mitochondrial substrates (Figure 1C), but their ability to utilize
89 those substrates decreased in cells infected with *B. abortus* (Figure 1D). This decrease
90 was dependent on MOI (Figures 1A). *Brucella*-infected cells, unlike with all other
91 substrates, continued to utilize glucose (Figure 1C–D). In fact, infected cells increased
92 glucose consumption with increasing MOI (Fig. S1).

93 The marked inhibition of mitochondrial substrate utilization suggests that
94 intracellular Brucellae diminish mitochondrial function. Parasites (7), viruses (8), and
95 intracellular bacterial pathogens including *B. melitensis* (9) and *Listeria monocytogenes*
96 (10) perturb mitochondrial function in host cells. To obtain additional evidence that
97 mitochondrial function is disrupted during *B. abortus* infection, we examined
98 mitochondrial morphology in uninfected and infected HeLa cells (because THP-1 cells
99 are not amenable to mitochondrial staining or imaging). Disruptions of mitochondrial
100 structure were observed in HeLa cells with detectable *B. abortus*, whereas uninfected
101 cells in the same field of view had normal cellular and mitochondrial morphology (Figure
102 2). Using an MTT cell viability assay we detected no loss in host viability with increasing
103 MOI within the same timeframe (Figure 1B). Therefore, it is unlikely that the
104 mitochondrial disruption observed by fluorescence microscopy results from host cell
105 death.

106 Most amino acids can be metabolized to enter the TCA cycle through anaplerotic
107 reactions (11). To determine whether the observed *B. abortus*-mediated disruption of
108 host mitochondrial function directly affects amino acid metabolism, we assessed the
109 effect of infection on the host's ability to utilize amino acids as a carbon source. While
110 glucose metabolism was unaffected, infected cells could not metabolize any of the
111 amino acids known to enter the TCA cycle (Figure 3). Together, the results of these
112 experiments are consistent with a model in which infection of human macrophages with
113 *B. abortus* results in major metabolic changes that are linked to disruption of
114 mitochondrial function.

115

116 ***Brucella*-dependent induction of lactic acid production in human cells**

117 Macrophages and dendritic cells are central to innate immunity. Upon activation, they
118 can undergo a shift in energy metabolism by shutting down oxidative phosphorylation
119 and increasing the rate of aerobic glycolysis in a process known as the Warburg effect
120 (3). A hallmark of this effect is production of lactic acid in the presence of oxygen. An
121 increase in lactate production in non-polarized macrophages infected with *Brucella* spp.
122 has been previously noted (12). To further validate that THP-1 infected with *B. abortus*-
123 are shifted toward a Warburg-like state, we measured the production of lactic acid in
124 host cells as a function of increasing MOI. THP-1 cells increase lactic acid production in
125 an MOI-dependent manner (Figure 4A). These results, together with the data presented
126 in Figures 1-3 support a model in which *Brucella* promotes a Warburg-like shift in host
127 cell metabolism by disrupting mitochondrial function.

128

129 ***Brucella abortus* lactate dehydrogenase is required for proper intracellular**
130 **replication**

131 *Brucella* and *Salmonella* both replicate intracellularly and can persist in the host for long
132 periods by shifting host metabolism to make glucose more available (12-14). We
133 measured the growth of *B. abortus* on two preferred substrates, glucose and erythritol,
134 and compared these data to growth on lactic acid. *B. abortus* grows on lactic acid as a
135 sole carbon and energy source as well as it does on glucose or erythritol in standing
136 culture *in vitro* (Figure 4B). We postulated that, during infection, *B. abortus* may exploit
137 the Warburg-type shift in host metabolism by utilizing lactic acid as a carbon and energy
138 source.

139 To define a genetic determinant of *B. abortus* lactic acid metabolism, we
140 engineered a strain harboring an in-frame deletion of the gene encoding L-lactate
141 dehydrogenase (LDH), *Bab2_0315* (Δ*lldD*). To determine whether *lldD* deletion affects
142 utilization of other carbon sources, we used PM to compare the metabolic activity of
143 Δ*lldD* to wild type (WT), and found that utilization of L-lactic acid was the most
144 statistically significant loss-of-function phenotype (Figure 5A). WT *B. abortus* exhibited
145 robust growth on lactic acid as a carbon and energy source, but Δ*lldD* did not grow in
146 this condition (Figure 5B). The Δ*lldD* mutant had no apparent growth defect in *Brucella*
147 broth supplemented with glucose (Figure 5C), but the numbers of colony forming units
148 (CFU) of Δ*lldD* were significantly reduced in THP-1 macrophages relative to WT at the
149 48-hour time point (Figure 5D). Complementation of the mutation by introduction of *lldD*

150 at its native locus rescued the THP-1 growth/replication defect. Together, our results
151 indicate that, upon infection, human cells increase lactic acid production and provide an
152 advantage to intracellular *B. abortus*, which can utilize host lactic acid as a carbon and
153 energy source.

154

155 **Small-molecule glycolysis inhibitors inhibit intracellular replication of *Brucella***
156 ***abortus* but do not inhibit axenic growth**

157 Identification of pathogen-induced changes in host metabolism offers new avenues for
158 the development of anti-infectives. Since *Brucella*-infected cells exhibited attenuated
159 mitochondrial function and increased glycolysis, we used small-molecule inhibitors of
160 glucose metabolism (Figure 6A) to determine whether inhibition of the host glycolytic
161 pathway affected intracellular growth/replication of *B. abortus*. We tested: 3-
162 bromopuruvic acid (3-BPA), an inhibitor of energy metabolism that completely
163 eradicated cancer in animal models with no apparent cytotoxicity (15, 16); methyl 1-
164 hydroxy-6-phenyl-4-(trifluoromethyl)-1H-indole-2-carboxylate (NHI-2), a potent
165 anticancer inhibitor of lactate dehydrogenase A (LDH-A) (17, 18); and 2-deoxy-D-
166 glucose (2-dG), a non-metabolizable homolog of D-glucose that slows glycolysis (19).

167 We counted *B. abortus* cells located inside THP-1 cells treated with each of
168 these anti-metabolic compounds at various concentrations. Since some of these
169 compounds may be toxic to cells at the tested concentrations, results were expressed
170 as the number of *Brucella* per THP-1 nucleus; hence, the data represent bacterial

171 counts in live cells only. Each anti-metabolic drug significantly inhibited
172 growth/replication of intracellular *Brucella* in live cells (Figure 6B).

173 To determine whether the antimicrobial activity of these compounds coincides
174 with their cytotoxicity to human cells, we assessed their cytotoxicity using an XTT cell
175 viability assay. As expected, each metabolic inhibitor was cytotoxic at higher
176 concentrations. Treatment of THP-1 cells with 3-BPA, the most potent compound,
177 inhibited *Brucella* infection at non-cytotoxic concentrations. NHI-2 and 2-dG were less
178 potent, but effectively inhibited growth/replication of intracellular *Brucella* (Figure 6C).
179 Both 3-BPA and NHI-2 significantly inhibited intracellular *Brucella* over a range of
180 concentrations that did not affect host cell viability.

181 Finally, to determine whether the antimicrobial effect of these compounds occurs
182 by host targeting, or whether they also directly inhibit bacterial growth, we measured
183 growth and viability of *B. abortus* in axenic culture in the presence of 3-BPA, NHI-2, and
184 2-dG. Neither 3-BPA nor NHI-2 affected growth and viability of *Brucella* in axenic
185 medium, though 2-dG exhibited an inhibitory effect at higher concentrations (≥ 50 mM).

186 These data support a model in which inhibition of host glycolysis and lactate
187 production with 3-BPA and NHI-2 inhibits intracellular *B. abortus* replication without
188 directly targeting *B. abortus* growth (Figure 6D). Together, these results demonstrate
189 that infection-induced changes in host central metabolic pathways are required for
190 proper growth/replication of intracellular *B. abortus*. Inhibition of the glycolytic pathway
191 with host-targeting anti-metabolic compounds provides an effective means to decrease
192 intracellular bacterial load without directly targeting the bacterium (Figure 6E).

193

194 **DISCUSSION**

195 We have identified metabolic changes in host cells upon exposure to an intracellular
196 bacterial pathogen, *B. abortus*. Intracellular *B. abortus* perturb the morphology and
197 function of host mitochondria, as characterized by loss of the ability to utilize
198 mitochondrial substrates (Figure 1 and 2). The host metabolic effects we observed upon
199 *B. abortus* infection resemble the effect of adding mitochondrial inhibitors (20), and are
200 consistent with the previously reported downregulation of mitochondrion-associated
201 gene expression in macrophages infected with *B. melitensis* (21). Many bacteria are
202 known to target host mitochondria (22), but only a few species have been reported to
203 disrupt mitochondrial morphology (9, 10, 23). The structures of mitochondria observed
204 in our study resemble those of cells treated with uncouplers in combination with a
205 respiration inhibitor; though this treatment resulted in energy deprivation and
206 aggregation of mitochondria, the cells remained viable (24).

207 Intracellular pathogens compete with the host cell for available nutrients,
208 including central metabolites and amino acids (25). As demonstrated using Biolog
209 mammalian PM, THP-1 cells utilized amino acids as an energy source, but this is
210 inhibited by *B. abortus* infection (Figure 3). The inability of infected cells to utilize amino
211 acids suggests that either intracellular Brucellae compete for the pool of available amino
212 acids, or the cells cease these catabolic reactions because of a change in mitochondrial
213 (or other) physiology. Inhibiting the TCA cycle and increasing glucose metabolism can
214 allow cells to rapidly generate the biomass required for cancer growth. Analogously,

215 induction of a Warburg-like state upon *B. abortus* infection may enable synthesis of
216 building blocks required for intracellular bacterial growth.

217 Intracellular pathogens rely on host resources for survival and replication. It is
218 therefore not surprising that other species of bacteria also affect host metabolism upon
219 infection. For example, *Mycobacterium tuberculosis* enhances glycolysis in THP-1 cells
220 (26). Early studies of the infection-induced changes in host metabolism showed that
221 cells infected with *Chlamydia* increase their utilization of glucose through glycolysis and
222 increase lactate production (27). Other pathogens, including the parasite *Plasmodium*
223 *falciparum* (28), and Mayaro virus (29), also induce similar changes in host metabolism.
224 Because the metabolic changes observed in these hosts are induced upon exposure to
225 various stimuli, it is unlikely that the changes observed in our study are specifically
226 induced by Brucellae.

227 Erythritol and glucose are preferred energy sources for *Brucella* (30), and our
228 results show that, in axenic culture, *Brucella* can utilize lactate as efficiently as erythritol
229 or glucose (Figure 4). Hence, we hypothesized that intracellular Brucellae can use
230 abundant host lactate as an energy source, which would enable successful intracellular
231 colonization and replication. We took two approaches to test whether host lactate
232 affects intracellular growth. First, we created a lactate dehydrogenase knockout strain
233 Δ*lldD*, which is unable to utilize lactate in axenic culture (Figure 5A-B). While Δ*lldD*
234 showed no growth defects across a range of axenic media, its intracellular
235 replication/survival was attenuated by ~1 log after 48 h in host THP-1 cells (Figure 5D).
236 This suggests that the ability to utilize lactate is necessary for proper replication in the

237 intracellular niche. We note there are parallels between *B. abortus* pathogenicity and
238 that of intracellular *Neisseria* spp., which is affected by host lactic acid (31). In the
239 second approach, we targeted host lactate synthesis using the small molecule inhibitors
240 NHI-2, 3-BPA, and 2-dG, which decrease lactate levels and inhibit aerobic glycolysis
241 (17, 18, 32, 33). Each of these metabolic inhibitors decreased intracellular growth
242 and/or replication of *Brucella* (Figure 6). Each of these compounds is known for its
243 anticancer properties, but their anti-infective properties were not previously reported.
244 Collectively, the data presented in this study support a model in which intracellular *B.*
245 *abortus* exploits host metabolic pathways (Figure 7). Hence, the host anti-metabolic
246 compounds identified here and in previous studies (34) may provide a novel therapeutic
247 approach to treat *B. abortus* and other bacterial infections that rely on host metabolic
248 intermediates.

249

250 **MATERIALS AND METHODS**

251 **Bacterial strains**

252 All studies on live *B. abortus* strain 2308 were conducted at Biosafety Level 3 (BSL3) at
253 the Howard Taylor Ricketts Regional Biocontainment Laboratory, University of Chicago,
254 according to US Federal Select Agent Program guidelines. *B. abortus* expressing
255 mCherry was previously generated from the WT *B. abortus* 2308 parent strain by
256 integrating mini-Tn7 expressing a single copy of *mCherry* at the *glmS* locus. Bacterial
257 strains used in this study are listed in Table S1.

258

259 **Mammalian tissue culture**

260 Prior to each experiment, THP-1 macrophage-like cells were grown to a maximum
261 density of 1 x 10^6 mL^{-1} in complete RPMI-1640 medium (HyClone) supplemented with
262 2 mM glutamine (Gibco) and 10% heat-inactivated fetal bovine serum (FBS) (HyClone).
263 HeLa cells were grown in Dulbecco Modified Eagles Medium (DMEM; HyClone)
264 supplemented with 10% heat-inactivated FBS. All tissue culture cells were grown at
265 37°C in a humidified environment with 5% CO_2.

266

267 **Mammalian Phenotype MicroArray: mitochondria toxicity**

268 THP-1 cells were seeded at 50,000 cells/well in two half-area 96-well plates in the
269 presence of 40 ng mL^{-1} phorbol myristate acetate (PMA), and allowed to differentiate
270 for 72 h at 37°C. *B. abortus* 2308 strain was streaked onto Schaedler blood agar (SBA)
271 plates before growing for 2 d, re-streaking, and growing for another 2 d. At the day of
272 infection, *Brucella* cells were scraped off the SBA plate, and suspended and washed in
273 RPMI-1640 growth medium. Cell concentration was measured by the optical density
274 method at 600 nm (OD_{600}). Bacteria were added to the last column of a 96-well plate at
275 1000 MOI, and serially diluted by a factor of two. The first column was left uninfected.
276 Plates were centrifuged at 2170 rpm for 10 min, followed by a 1-h incubation at 37°C
277 and 5% CO_2. Gentamicin was added to each well at a final concentration of
278 100 µg mL^{-1} and the plates were further incubated for 1 h. Following incubation, the

279 medium was removed and replaced with fresh medium containing 25 μg mL^{-1}
280 gentamicin. Cells were incubated for 24 h. Twenty-four hours after infection, two PM-M
281 TOX1 MicroPlates (Biolog) were reconstituted with 50 μL (per well) of MC-0 medium
282 (Biolog IF-M1 medium, 0.3 mM L-Gln, 5% dialyzed FBS, 25 μg mL^{-1} gentamicin). The
283 culture medium was removed from infected cells and replaced with the contents of
284 reconstituted PM-M TOX1 plates. *Brucella*-infected cells were incubated in the presence
285 of mitochondrial substrates for another 24 h. Following this incubation, 10 μL of PM-A
286 dye (Biolog) was added to each well, and the absorbance measured every 15 min (up to
287 150 min) at 590 nm and 750 nm using a Tecan Infinite 200 PRO microplate reader.
288 Plates were incubated at 37°C and 5% CO_2 between readings. The collected
289 absorbance 590 nm data (minus reference absorbance at 750 nm) were analyzed as a
290 function of time.

291 Following the experiment, cell viability was assessed by removing all liquid from
292 the PM-M TOX1 plate, replacing it with glucose-supplemented growth medium
293 containing 10% FBS, and 0.5 mg mL^{-1} MTT reagent, then measuring the absorbance at
294 570 nm after 24 h.

295

296 **Mammalian Phenotype MicroArray: utilization of amino acids**

297 THP-1 and *B. abortus* 2308 cells were prepared as described above. The infection
298 protocol was as described above with small changes. Bacteria were added to
299 differentiated THP-1 cells in a 96-well plate at 100 MOI. Plates were centrifuged at
300 2170 rpm for 10 min followed by 1-h incubation at 37°C and 5% CO_2. Gentamicin was

301 added to each well at a final concentration of 100 μg mL^{-1} and plates were further
302 incubated for 1 h. Following incubation, the medium was removed and replaced with a
303 fresh medium containing 25 μg mL^{-1} gentamicin. Cells were incubated for 24 h. Twenty-
304 four hours after infection, the content of the mammalian phenotype microarray PM-M2
305 (Biolog) was reconstituted with 50 μL (per well) of MC-0 medium (Biolog IF-M1 medium,
306 0.3 mM L-Gln, 5% dialyzed FBS, 25 μg mL^{-1} gentamicin). The culture medium was
307 removed from infected cells and replaced with the contents of reconstituted PM-M2
308 plates. *Brucella*-infected cells were incubated in the presence of various amino acids for
309 another 24 h. Following this incubation, 10 μL of dye PM-A (Biolog) was added to each
310 well, and the absorbance was measured every 15 min (up to 120 min) at 590 nm and
311 750 nm using a Tecan Infinite 200 PRO microplate reader. Plates were incubated at
312 37°C and 5% CO_2 between readings. Absorbance at 590 nm data (minus reference
313 absorbance at 750 nm) was analyzed as a function of time. Results were analyzed by
314 hierarchical clustering using Gene Cluster 3.0 and visualized using Java TreeView
315 (v1.1.6r4).

316

317 **Bacterial Phenotype MicroArray**

318 Utilization of glucose, erythritol, and lactic acid was measured using PM as previously
319 described (35). Briefly, *B. abortus* strains (WT 2308 and Δ*bab2_0315*) were streaked
320 onto an SBA plate, cultivated at 37°C and 5% CO_2 for 48 h, re-streaked, and grown for
321 another 48 h. Cells were scraped off the plate and resuspended in 1 x IF-0a medium
322 (Biolog) at a final density equivalent to 5% transmittance (OD_{600nm}). PM inoculating

323 fluids (PM1 and PM2) were prepared from 0.2-μm-filtered and sterilized stock solutions
324 at the following final concentrations: 2 mM $MgCl_2$, 1 mM $CaCl_2$, 25 μM L-arginine,
325 50 μM L-glutamic acid, 5 μM β-NAD, 25 μM hypoxanthine, 25 μM 5′-UMP, 25 μM L-
326 cystine (pH 8.5), 0.005% yeast extract, and 0.005% Tween 40. PM1 and PM2
327 inoculating fluids were prepared in 1 x IF-0a GN/GP medium (Biolog). Dye mix G
328 (Biolog) was added to each solution to a final concentration of 1X. A 1:13.6 dilution of
329 5% transmittance *Brucella* suspension was added to each inoculating fluid. Per well,
330 100 μL of *Brucella*-containing inoculating fluid was dispensed into each PM plate. PM
331 plates were incubated at 37°C and 5% CO_2, and the absorbance at 630 nm was
332 measured every 24 h for up to 5 d, using a Tecan Infinite 200 PRO microplate reader.

333

334 **Imaging of mitochondria**

335 HeLa cells were seeded onto 22 x 22 mm cover slides at 50,000 cells/well in a 6-well
336 plate in 2 mL of DMEM medium per well. Cells were grown for 24 h prior to infection.
337 Prior to infection, a culture of *B. abortus* constitutively expressing mCherry was
338 inoculated in *Brucella* broth, and grown overnight at 37°C on orbital shaker. On the day
339 of infection, *Brucella* cells were collected, resuspended in DMEM, and opsonized by
340 incubating for 30 min at 37°C with 1:1000 dilution of serum obtained from *Brucella*-
341 infected mice, as previously described (36). Following opsonization, cells were washed
342 and added to HeLa cells at 10,000 MOI. The plate was centrifuged at 2170 rpm for
343 20 min, and placed for 24 h at 37°C and 5% CO_2. Following incubation, cells were
344 washed with DMEM, re-infected at 10,000 MOI, and incubated for another 24 h. After

345 this incubation, cells were washed with DMEM, the cover slide was transferred to a
346 50 mL tube containing 15 mL DMEM and 200 μg mL^{-1} gentamicin. The slide was
347 incubated at 37°C and 5% CO_2 for 1 h. Following the incubation, 15 μL of 10 mg mL^{-1}
348 Hoechst stain and 2 μL of 1 mM MitoTracker (Molecular Probes) dye were added and
349 incubated for another 20 min. The cover slide was washed and placed on a microscope
350 slide with cells facing up. A drop of DMEM was placed on top of the cover slide and
351 covered by another 22 x 22 mm cover slide. To prevent medium evaporation, the edges
352 were quickly sealed with nail polish, and live cells were immediately imaged using a
353 Leica-DMI6000B fluorescence microscope equipped with a HC PL APO 63X/1.4 NA Oil
354 PH3 CS2 objective. Images were captured using Leica Application Suite X and
355 Hamamatsu Orca-R2 camera.

356 **Quantification of lactic acid**

357 Intracellular lactic acid levels were quantified according to the manufacturer's protocol
358 using a lactate assay kit (Sigma-Aldrich). Briefly, THP-1 cells were seeded and infected
359 with *B. abortus* at increasing MOI, as described above. Infected cells were incubated for
360 48 h before quantifying lactate levels. After incubation, cells were washed with PBS,
361 homogenized in 60 μL of lactate assay buffer, and cell debris was removed by
362 centrifuging at 14,000 *g* for 10 min. Fifty microliters of supernatant was collected from
363 each sample, and endogenous lactate dehydrogenase was removed by centrifuging
364 supernatants at 14,000 *g* for 30 min using 10 kDa MWCO Ultra-0.5 mL spin filter
365 (Amicon). Twenty microliters of lactate assay buffer was added to each sample to bring
366 the volume up to 50 μL. Fifty microliters of master mix (lactate assay buffer, enzyme

367 mix, and probe) was added to each well, mixed, and incubated in the dark at room
368 temperature for 30 min before measuring absorbance at 570 nm. Lactate concentration
369 was calculated based on a standard lactate curve and normalized to the number of cells
370 per well.

371 **Construction of *B. abortus lldD* chromosomal deletion**

372 A chromosomal deletion of *B. abortus lldD* (*bab2_0315*) was obtained using a double
373 recombination strategy. Primers used in this study are given in Table S2. The 500 base
374 pairs upstream (using primers 1775 and 1779) and downstream (using primers 1776
375 and 1777) of *lldD* were Gibson-cloned into pNPTS138, which was digested with *Bam*HI
376 and *Hin*dIII (New England Biolabs). Constructs were validated by DNA sequencing. To
377 delete *lldD*, the deletion plasmid was transformed into *B. abortus*, and primary
378 integrants were selected by plating on SBA supplemented with 50 µg mL^{-1} kanamycin
379 (SBA-Kan). The resulting colonies were grown overnight in *Brucella* broth without
380 selection and plated on SBA supplemented with 5% sucrose to select for second
381 crossovers. The resulting colonies were screened for the *lldD* deletion by sequencing
382 using the sequencing primers 1788/1789.

383 To complement the *lldD* deletion strain, the *lldD* gene plus the 500 bp upstream
384 and downstream (using primers 1775/1777) were Gibson-cloned into pNPTS138, and
385 restored at the native site using a two-step recombination strategy as outlined above.

386

387 ***Brucella* axenic growth**

388 The concentration of *Brucella* cells (WT 2308 and Δ*bab2_0315*) was adjusted to 20%
389 transmittance at OD_{600} and diluted into glucose-containing *Brucella* broth (Difco) at 1:20.
390 MTT (3-(4.5-dimethylthiazol-2-yl)-2.5-diphenyltetrazolium bromide) reagent was added
391 to the media to a final concentration of 0.5 mg mL^{-1}, and cells were continuously
392 incubated at 37°C in a Tecan plate reader, taking absorbance readings at 570 nm every
393 10 min for 72 h.

394

395 ***Brucella* axenic growth: compound cytotoxicity**

396 NHI-2 (Sigma-Aldrich), 3-BPA, and 2-dG (Santa Cruz Biotechnology) were freshly
397 prepared and serially diluted to test concentrations in a half-area 96-well plate in a total
398 volume of 50 µL of PM9 medium (2 mM $MgCl_2$• $6H_20$, 1 mM $CaCl_2$• $2H_2O$, 0.005% yeast
399 extract, 0.005% Tween 40, 2.5 mM D-glucose, 5 mM sodium pyruvate, and 1X Dye Mix
400 G [Biolog]). WT 2308 *Brucella* was prepared from a plate culture in PM9 medium at
401 20% transmission at 600 nm optical density, and 50 µL was added to each well for a
402 total volume of 100 µL per well. Cells were incubated at 37°C, and absorbance at
403 630 nm was read every 2 h for 72 h using a Tecan microplate reader.

404

405 **XTT cell viability assay**

406 The cytotoxicity of NHI-2, 3-BPA, and 2-dG to THP-1 cells was assessed using the XTT
407 cell proliferation and viability assay kit (Roche), according to the supplier's protocol.
408 Briefly, cells were seeded at 50,000 cells/well. Various concentrations of compounds

409 were added to each well, in triplicate, in the presence of 25 µg mL^{-1} of gentamicin. Cells
410 were incubated for 72 h before measuring viability using the XTT assay. XTT reagents
411 were prepared according to the manufacturer's instructions. Following incubation, 50 µL
412 of XTT labeling mixture was added per well, and cells were further incubated for 4 h at
413 37°C and 5% CO_2. Absorbance measurements were collected at 590 nm and 750 nm
414 (reference wavelength). Final data were expressed as absorbance readings at 590 nm
415 (minus 750 nm reference absorbance) at the respective compound concentrations.

416

417 **Quantifying *Brucella* infection of THP-1 cells**

418 THP-1 cells were seeded in a black-well, clear-bottom 96-well plate (Costar) at 50,000
419 cells/well, differentiated with 40 ng mL^{-1} PMA for 72 h. Two hours before infection, cells
420 were treated with compounds, and infected with *B. abortus* at 100 MOI, as described
421 above. Fresh compounds were added back into media containing 25 µg mL^{-1}
422 gentamicin, and cells were further incubated for 72 h. After incubation, cells were
423 washed three times with 1X PBS, and fixed for 10 min with 4% paraformaldehyde,
424 followed by three washes with 1X PBS. Cell nuclei were labeled with 1 µg mL^{-1} Hoechst
425 stain. Cells were imaged using a Leica-DMI6000B fluorescence microscope equipped
426 with a 20X/0.4 NA objective, Hamamatsu Orca-R2 camera, and Leica Application Suite
427 X. Forty images were captured in four replicate experiments: ten images per condition
428 per replicate. Cell Profiler (v2.1.1) was used to measure the number of intracellular
429 fluorescent Brucellae, and the number of THP-1 nuclei. The effect of the compounds on
430 *B. abortus* intracellular growth was assessed by calculating the number of bacteria per
431 cell, represented as a ratio of the total number of bacteria to the total number of nuclei

432 (*Brucella* per THP-1 nucleus) per image, which was calculated as an average of 40
433 images ± standard error of the mean. Statistical significance was determined using one-
434 way analysis of variance (ANOVA) followed by Dunnett's test.

435 To enumerate CFU at 1, 24, and 48 hours post-infection of THP-1, *B. abortus*
436 cells were resuspended in warmed RPMI and added at a multiplicity of infection (MOI)
437 of 100 CFU per macrophage cell. To synchronize infections after the addition of
438 *Brucella* cells, plates were centrifuged at 200 x *g* for 5 minutes. After a 30-minute
439 incubation, media was removed and replaced with RPMI supplemented with 100 µg mL^{-}
440 ^{1} gentamycin to kill extracellular bacteria. Afterwards, samples were incubated for 1
441 hour, after which monolayers were washed with PBS and THP-1 cells were lysed by
442 addition of 0.01% Triton X-100. Serial dilutions were prepared and viable cells were
443 determined by plating on TSA plates. For longer time points, the RPMI was removed,
444 and replaced with RPMI supplemented with 50 µg mL^{-1} gentamycin. Additional samples
445 were lysed as above and serial dilutions plated. All THP-1 assays were performed in
446 triplicate utilizing independent *B. abortus* cultures.

447

448 **ACKNOWLEDGEMENTS**

449 We acknowledge the support staff of the Howard Taylor Ricketts Regional
450 Biocontainment Laboratory. We also acknowledge and thank Barry Bochner and Aretha
451 Fiebig for thoughtful feedback and critical evaluation of the manuscript. This study was
452 funded in part by National Institutes of Health grant R01AI107159 to SC, and the

453 Chicago Biomedical Consortium with support from the Searle Funds at the Chicago
454 Community Trust.

455

456 **AUTHOR CONTRIBUTIONS**

457 DC and SC conceived and designed the experiments, analyzed the data, and wrote the
458 manuscript. DC and JW performed the experiments. All authors reviewed and approved
459 the final manuscript.

460

461 **REFERENCES**

462 1. **Galvan-Pena S, O'Neill LA.** 2014. Metabolic reprograming in macrophage
463 polarization. Front Immunol **5:**420.
464 2. **Pearce EL, Pearce EJ.** 2013. Metabolic pathways in immune cell activation and
465 quiescence. Immunity **38:**633-643.
466 3. **Kelly B, O'Neill LA.** 2015. Metabolic reprogramming in macrophages and
467 dendritic cells in innate immunity. Cell Res **25:**771-784.
468 4. **Warburg O, Wind F, Negelein E.** 1927. The metabolism of tumors in the body. J
469 Gen Physiol **8:**519-530.
470 5. **Bedard K, Krause KH.** 2007. The NOX Family of ROS-Generating NADPH
471 Oxidases: Physiology and Pathophysiology. Physiol Rev **87:**245-313.
472 6. **Nathan CF, Hibbs JB.** 1991. Role of nitric oxide synthesis in macrophage
473 antimicrobial activity. Curr Opin Immunol **3:**65-70.
474 7. **Luckhart S, Pakpour N, Giulivi C.** 2015. Host-pathogen interactions in malaria:
475 cross-kingdom signaling and mitochondrial regulation. Curr Opin Immunol **36:**73-
476 79.
477 8. **Koshiba T.** 2013. Mitochondrial-mediated antiviral immunity. Biochim Biophys
478 Acta **1833:**225-232.
479 9. **Li T, Xu Y, Liu L, Huang M, Wang Z, Tong Z, Zhang H, Guo F, Chen C.** 2016.
480 *Brucella Melitensis* 16M Regulates the Effect of AIR Domain on Inflammatory
481 Factors, Autophagy, and Apoptosis in Mouse Macrophage through the ROS
482 Signaling Pathway. PLoS One **11:**e0167486.

483 10. **Stavru F, Bouillaud F, Sartori A, Ricquier D, Cossart P.** 2011. *Listeria*
484 *monocytogenes* transiently alters mitochondrial dynamics during infection. Proc
485 Natl Acad Sci U S A **108:**3612-3617.
486 11. **Owen OE, Kalhan SC, Hanson RW.** 2002. The Key Role of Anaplerosis and
487 Cataplerosis for Citric Acid Cycle Function. J Biol Chem **277:**30409-30412.
488 12. **Xavier MN, Winter MG, Spees AM, den Hartigh AB, Nguyen K, Roux CM,**
489 **Silva TMA, Atluri VL, Kerrinnes T, Keestra AM, Monack DM, Luciw PA,**
490 **Eigenheer RA, Bäumler AJ, Santos RL, Tsolis RM.** 2013. PPARγ-Mediated
491 Increase in Glucose Availability Sustains Chronic *Brucella abortus* Infection in
492 Alternatively Activated Macrophages. Cell Host Microbe **14:**159-170.
493 13. **Roop RM, Caswell CC.** 2013. Bacterial Persistence: Finding the "Sweet Spot".
494 Cell Host Microbe **14:**119-120.
495 14. **Eisele NA, Ruby T, Jacobson A, Manzanillo PS, Cox JS, Lam L, Mukundan**
496 **L, Chawla A, Monack DM.** 2013. *Salmonella* Require the Fatty Acid Regulator
497 PPARδ for the Establishment of a Metabolic Environment Essential for Long-
498 Term Persistence. Cell Host Microbe **14:**171-182.
499 15. **Cardaci S, Desideri E, Ciriolo MR.** 2012. Targeting aerobic glycolysis: 3-
500 bromopyruvate as a promising anticancer drug. J Bioenerg Biomembr **44:**17-29.
501 16. **Ko YH, Smith BL, Wang Y, Pomper MG, Rini DA, Torbenson MS, Hullihen J,**
502 **Pedersen PL.** 2004. Advanced cancers: eradication in all cases using 3-
503 bromopyruvate therapy to deplete ATP. Biochem Biophys Res Comm **324:**269-
504 275.

505 17. **Granchi C, Calvaresi EC, Tuccinardi T, Paterni I, Macchia M, Martinelli A,**
506 **Hergenrother PJ, Minutolo F.** 2013. Assessing the differential action on cancer
507 cells of LDH-A inhibitors based on the N-hydroxyindole-2-carboxylate (NHI) and
508 malonic (Mal) scaffolds. Org Biomol Chem **11:**10.1039/c1033ob40870a.
509 18. **Calvaresi EC, Granchi C, Tuccinardi T, Di Bussolo V, Huigens RW, Lee HY,**
510 **Palchaudhuri R, Macchia M, Martinelli A, Minutolo F, Hergenrother PJ.** 2013.
511 Dual Targeting of the Warburg Effect with a Glucose-Conjugated Lactate
512 Dehydrogenase Inhibitor. Chembiochem **14:**2263-2267.
513 19. **Wick AN, Drury DR, Nakada HI, Wolfe JB.** 1957. Localization of the primary
514 metabolic block produced by 2-deoxyglucose. J Biol Chem **224:**963-969.
515 20. **Bochner BR, Siri M, Huang RH, Noble S, Lei XH, Clemons PA, Wagner BK.**
516 2011. Assay of the multiple energy-producing pathways of mammalian cells.
517 PLoS One **6:**e18147.
518 21. **He Y, Reichow S, Ramamoorthy S, Ding X, Lathigra R, Craig JC, Sobral BW,**
519 **Schurig GG, Sriranganathan N, Boyle SM.** 2006. *Brucella melitensis* triggers
520 time-dependent modulation of apoptosis and down-regulation of mitochondrion-
521 associated gene expression in mouse macrophages. Infect Immun **74:**5035-
522 5046.
523 22. **Lobet E, Letesson JJ, Arnould T.** 2015. Mitochondria: A target for bacteria.
524 Biochem Pharmacol **94:**173-185.
525 23. **Ma C, Wickham ME, Guttman JA, Deng W, Walker J, Madsen KL, Jacobson**
526 **K, Vogl WA, Finlay BB, Vallance BA.** 2006. *Citrobacter rodentium* infection
527 causes both mitochondrial dysfunction and intestinal epithelial barrier disruption

528 in vivo: role of mitochondrial associated protein (Map). Cell Microbiol **8:**1669-
529 1686.
530 24. **Lyamzaev KG, Pletjushkina OY, Saprunova VB, Bakeeva LE, Chernyak BV,**
531 **Skulachev VP.** 2004. Selective elimination of mitochondria from living cells
532 induced by inhibitors of bioenergetic functions. Biochem Soc Trans **32:**1070-
533 1071.
534 25. **Abu Kwaik Y, Bumann D.** 2015. Host Delivery of Favorite Meals for Intracellular
535 Pathogens. PLoS Pathog **11:**e1004866.
536 26. **Mehrotra P, Jamwal SV, Saquib N, Sinha N, Siddiqui Z, Manivel V,**
537 **Chatterjee S, Rao KV.** 2014. Pathogenicity of *Mycobacterium tuberculosis* is
538 expressed by regulating metabolic thresholds of the host macrophage. PLoS
539 Pathog **10:**e1004265.
540 27. **Moulder JW.** 1970. Glucose Metabolism of L Cells Before and After Infection
541 with *Chlamydia psittaci*. J Bacteriol **104:**1189-1196.
542 28. **Mehta M, Sonawat HM, Sharma S.** 2005. Malaria parasite-infected erythrocytes
543 inhibit glucose utilization in uninfected red cells. FEBS Letters **579:**6151-6158.
544 29. **El-Bacha T, Menezes MMT, Azevedo e Silva MC, Sola-Penna M, Da Poian**
545 **AT.** 2004. Mayaro virus infection alters glucose metabolism in cultured cells
546 through activation of the enzyme 6-phosphofructo 1-kinase. Mol Cell Biochem
547 **266:**191-198.
548 30. **Anderson JD, Smith H.** 1965. The Metabolism of Erythritol by *Brucella Abortus*.
549 J Gen Microbiol **38:**109-124.

550 31. **Smith H, Tang CM, Exley RM.** 2007. Effect of Host Lactate on Gonococci and
551 Meningococci: New Concepts on the Role of Metabolites in Pathogenicity. Infect
552 Immun **75:**4190-4198.
553 32. **El Sayed SM, El-Magd RM, Shishido Y, Chung SP, Diem TH, Sakai T,**
554 **Watanabe H, Kagami S, Fukui K.** 2012. 3-Bromopyruvate antagonizes effects
555 of lactate and pyruvate, synergizes with citrate and exerts novel anti-glioma
556 effects. J Bioenerg Biomembr **44:**61-79.
557 33. **Barban S, Schulze HO.** 1961. The Effects of 2-Deoxyglucose on the Growth and
558 Metabolism of Cultured Human Cells. J Biol Chem **236:**1887-1890.
559 34. **Czyz DM, Jain-Gupta N, Shuman HA, Crosson S.** 2016. A dual-targeting
560 approach to inhibit Brucella abortus replication in human cells. Sci Rep **6:**35835.
561 35. **Herrou J, Czyż DM, Willett JW, Kim HS, Chhor G, Babnigg G, Kim Y,**
562 **Crosson S.** 2016. WrpA Is an Atypical Flavodoxin Family Protein under
563 Regulatory Control of the *Brucella abortus* General Stress Response System. J
564 Bacteriol **198:**1281-1293.
565 36. **Kim HS, Caswell CC, Foreman R, Roop RM, Crosson S.** 2013. The *Brucella*
566 *abortus* General Stress Response System Regulates Chronic Mammalian
567 Infection and Is Controlled by Phosphorylation and Proteolysis. J Biol Chem
568 **288:**13906-13916.

569

570

571

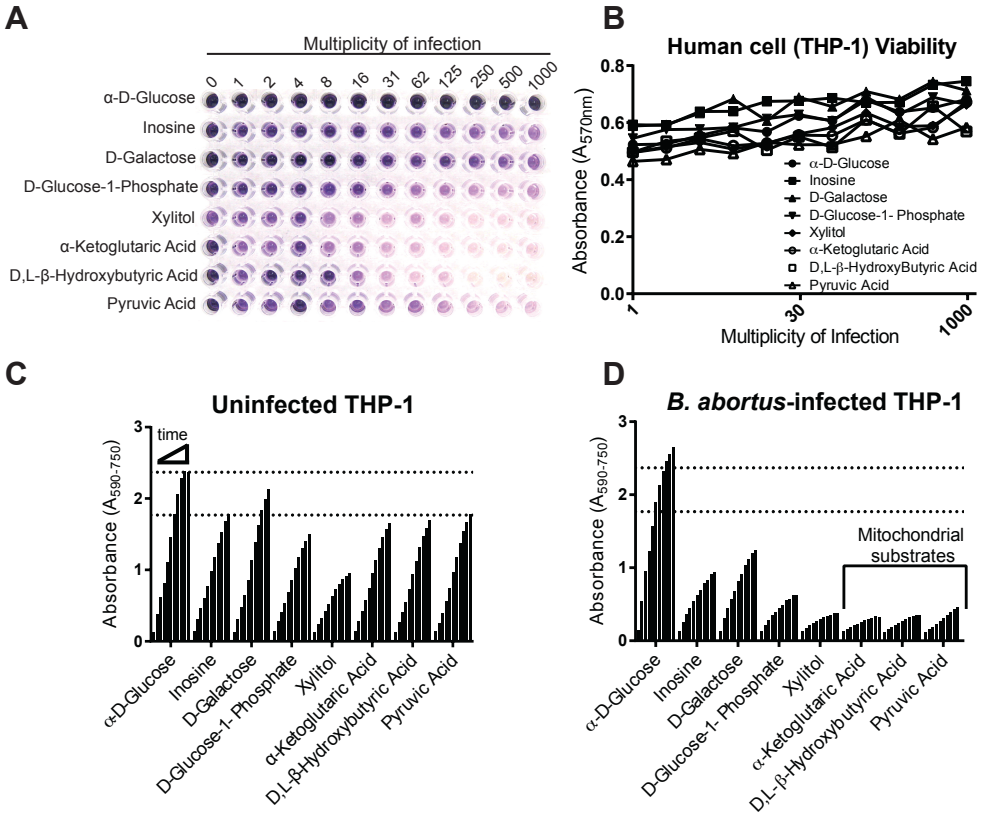

572

573 **FIG 1. Mitochondrial function is perturbed in THP-1 cells infected with *B. abortus.***

574 **(A)** Mammalian Phenotype MicroArray (PM) plate designed to measure mitochondrial
575 function. The ability of THP-1 cells infected with *B. abortus* at increasing multiplicity of
576 infection (MOI) to utilize metabolic substrates was assessed by measuring the reduction
577 of a tetrazolium dye (see Materials and Methods). **(B)** An MTT cell viability assay was
578 performed in the presence of glucose to assess the effect of *B. abortus* infection on
579 human cell survival at the conclusion of the mammalian PM assay. Dye reduction by **(C)**
580 uninfected and **(D)** *Brucella*-infected human cells (MOI 125) measured as a time-
581 dependent absorbance readout. Cells were cultured in minimal medium supplemented
582 either with glucose (control) or central metabolic substrates. Brackets indicate
583 substrates (α-ketoglutaric acid, β-hydroxybutyric acid, and pyruvic acid), which enter the

584 mitochondria, thereby providing a direct readout of mitochondrial function. Bars along
585 the X axes represent time (0–150 min) in 15-min increments. Dotted lines mark the
586 highest reading for utilization of glucose and pyruvic acid in uninfected THP-1 cells.

587

588 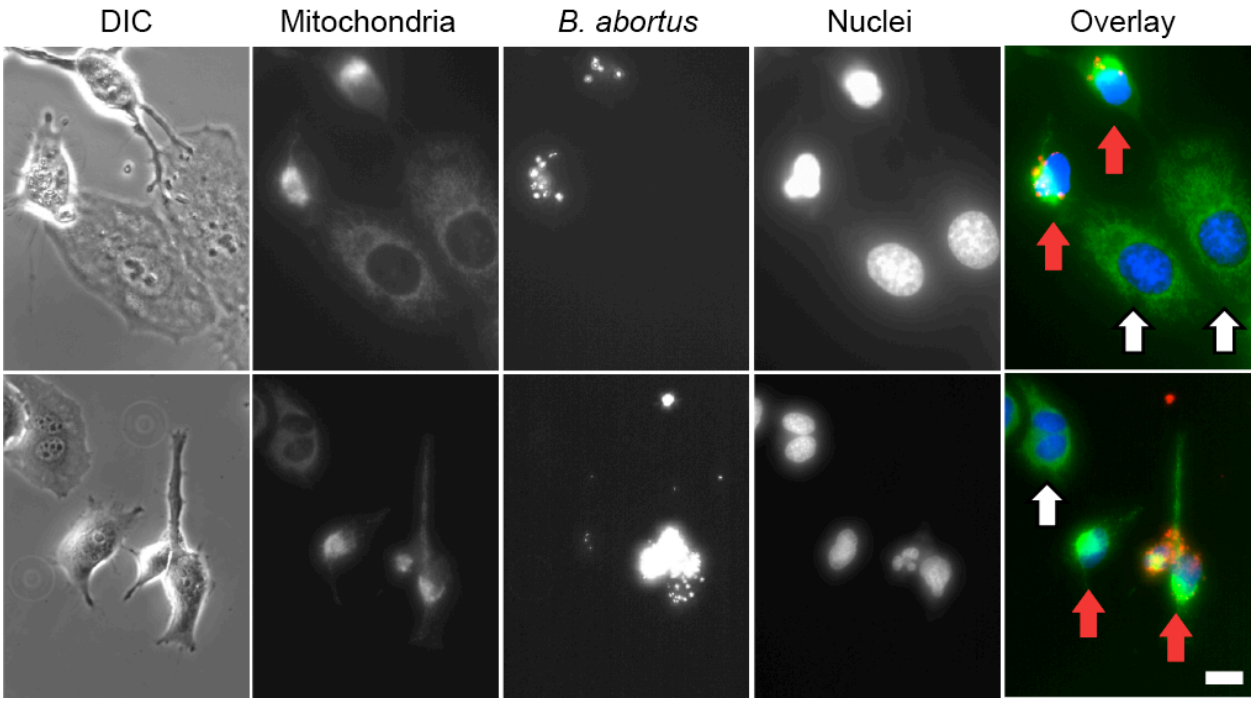

589 **FIG 2. Intracellular *B. abortus* induces morphological changes of mitochondria in**
590 **HeLa cells.**

591 Two fields showing mitochondrial staining (MitoTracker, green), *B. abortus*-Tn7mCherry
592 (mCherry fluorescence, red), nuclei (Hoechst stain, blue), and the corresponding image
593 with differential interference contrast (DIC) microscopy. Red arrows indicate cells with
594 visible intracellular *B. abortus*, white arrows indicate cells for which no infection is
595 evident. Cells not infected with *B. abortus* have typical morphology and mitochondrial
596 structure. Scale bar = 50 µm.

597

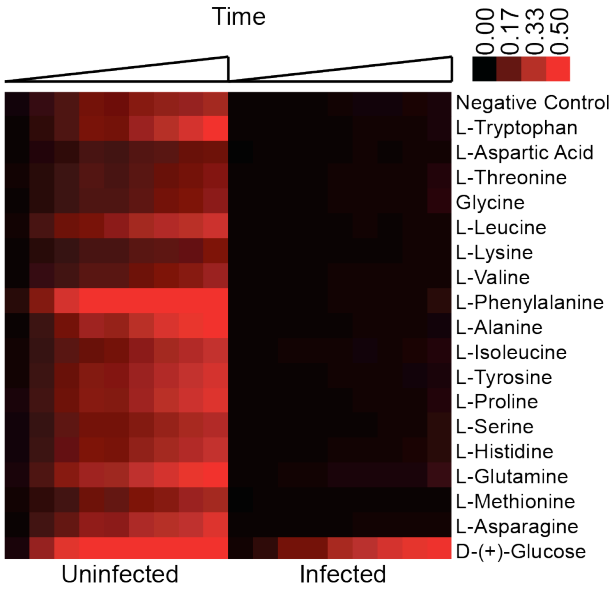

FIG 3. Host cell utilization of amino acids as a carbon source before and after *B. abortus* infection.

Heatmap representing host cell metabolism as measured colorimetrically via a redox dye (see Materials and Methods). Time-dependent metabolic change of non-infected versus *B. abortus*-infected THP-1 cells in the presence of amino acids are plotted. Color is an arbitrary scale from black (no reduction of the dye, 0.00) to red (maximum reduction of the dye, 0.50).

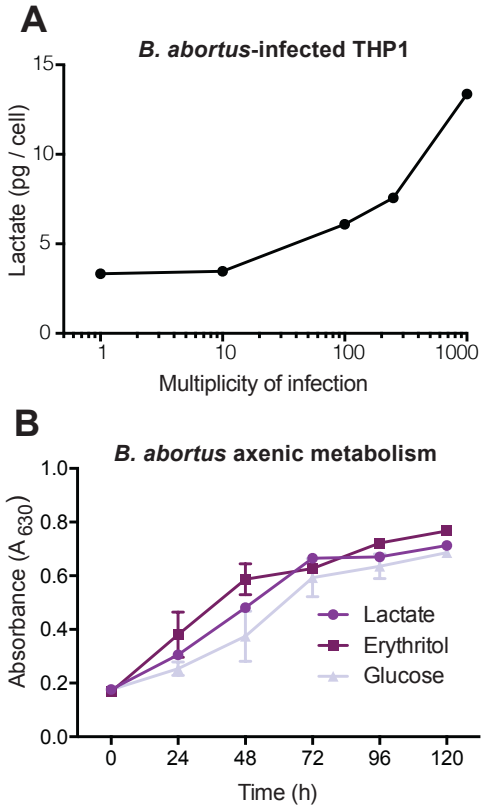

607

608 **FIG 4. *B. abortus* induces host cell lactate production and utilizes lactate as a**
609 **carbon and energy source as efficiently as glucose and erythritol.**

610 **(A)** Lactate levels in THP-1 cells upon infection with *B. abortus* at different multiplicities
611 of infection. **(B)** Metabolism of *B. abortus* measured on carbon/energy sources lactate,
612 erythritol, or glucose. Data show an average of two independent experiments ±
613 standard deviation.

614

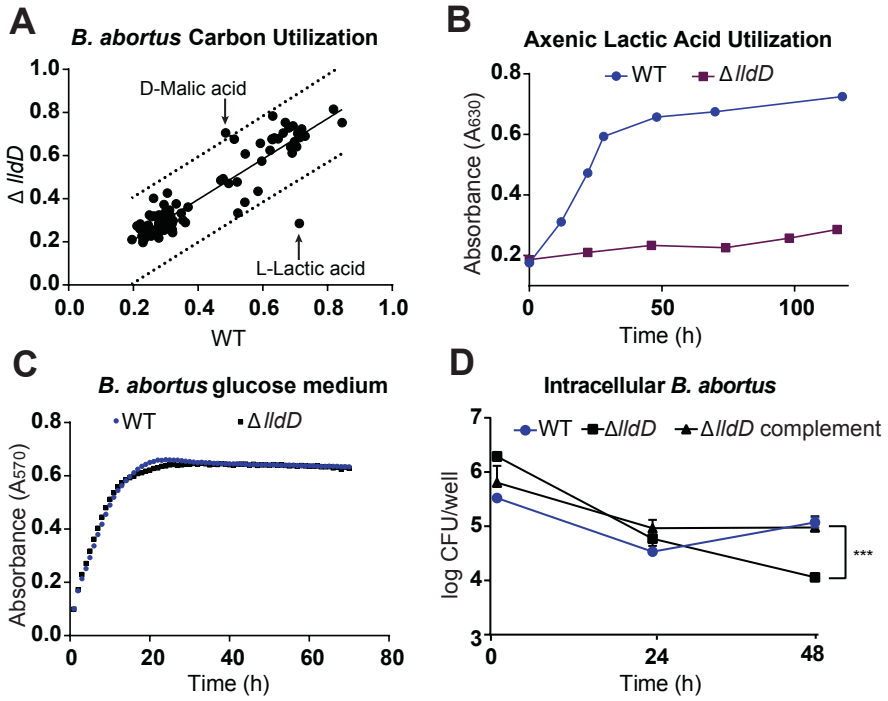

615

616 **FIG 5. *B. abortus* L-lactate dehydrogenase deletion strain Δ*lldD* cannot utilize**
617 **lactic acid in axenic culture and is attenuated in a macrophage infection model.**

618 **(A)** Phenotype MicroArray carbon utilization measurements of wild-type (WT) *B. abortus*
619 and L-lactate dehydrogenase (LDH) mutant (Δ*lldD*) strains. Metabolic activities for
620 growth on 95 distinct carbon substrates (see Materials and Methods) are plotted against
621 each other; the dotted line marks a 99% prediction band of a linear regression.
622 Correlation values above the line represent a gain-of-function phenotype and values
623 below the line represent a loss-of-function phenotype. L-lactic acid and D-malic acid are
624 marked as loss-of-function and gain-of-function, respectively **(B)** Graph representing
625 time-dependent utilization of lactic acid as a carbon energy source, and measured by a
626 metabolic indicator dye (see Materials and Methods). **(C)** Graph representing axenic
627 growth of the WT and Δ*lldD* strains in glucose-containing *Brucella* broth. **(D)** Intracellular

628 replication of the WT and Δ*lldD* strains in macrophage cell infection model. Intracellular
629 Brucellae were quantified as $\log_{10}$ colony forming units (CFU) per well at 1, 24, and 48 h
630 post-infection. Lines represent WT (●), Δ*lldD* mutant (■), and complement (▲). n=3,
631 Error bars represent standard deviation.

632

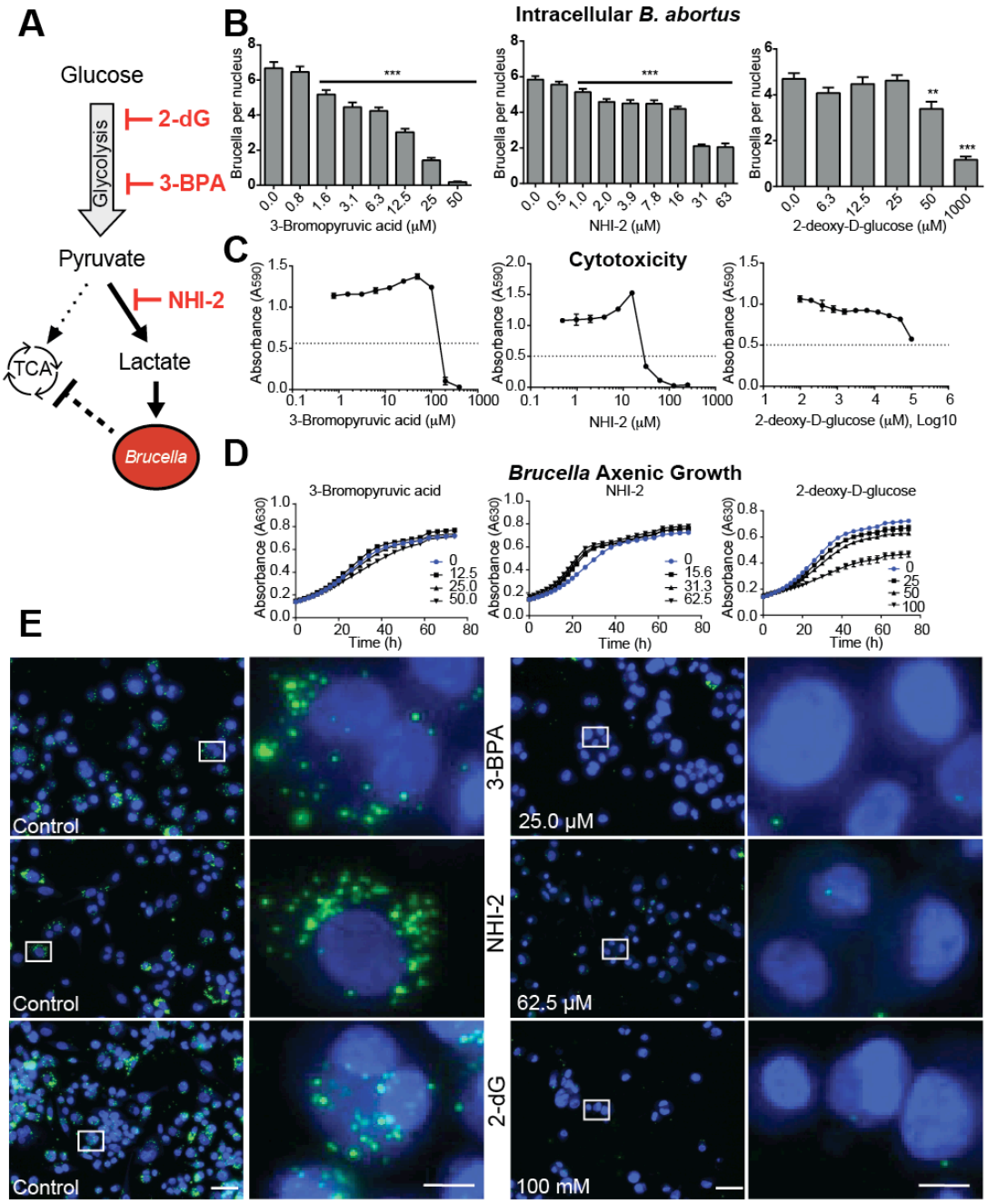

633

634 **FIG 6. Pharmacological disruption of the host glycolytic pathway and lactate**

635 **production inhibits replication of intracellular *B. abortus*.**

636 **(A)** Model depicting *Brucella*-dependent modulation of carbon metabolism and
637 activation of aerobic glycolysis, resulting in the production of lactate. *B. abortus* utilizes
638 lactate as efficiently as preferred substrates glucose and erythritol. Pharmacological
639 inhibitors of glycolysis, 3-Bromopyruvic acid (3-BPA), NHI-2, and 2-deoxy-D-glucose (2-
640 dG), inhibit intracellular growth of *B. abortus*: **(B)** Graphs represent the effect of 3-BPA,
641 NHI-2, and 2-dG on intracellular replication of *B. abortus* as quantified by enumerating
642 fluorescent bacteria per THP-1 nucleus; **(C)** cytotoxicity of inhibitory compounds to
643 THP-1 cells, and **(D)** effect of metabolic inhibitors on *B. abortus* axenic
644 growth/metabolism. The effect of anti-glycolytic compounds on infection was assessed
645 by measuring the average ratio of bacteria-to-nuclei in THP-1 cells treated with each of
646 the compounds. Statistical significance was evaluated from four biological replicates (10
647 images each) using one-way analysis of variance (ANOVA) followed by Dunnett's post
648 test $^{**}p < 0.01$, $^{***}p < 0.0001$). Error bars represent ± standard deviation from the mean;
649 an XTT assay was used to measure compound cytotoxicity to THP-1 cells; *Brucella*
650 axenic growth/metabolism was assayed by measuring tetrazolium-based dye reduction
651 at 630 nm **(E)** Fluorescence images of nuclei (blue) and intracellular *B. abortus*
652 (pseudocolored green) reflect the efficacy of 3-BPA, NHI-2, and 2-dG to inhibit *B.*
653 *abortus* replication in the intracellular niche. Scale bars = 10 μm (full view) and 50 μm
654 (magnified insets, marked with white box in full view). Dotted line = half maximal
655 inhibitory concentration (IC50).

656

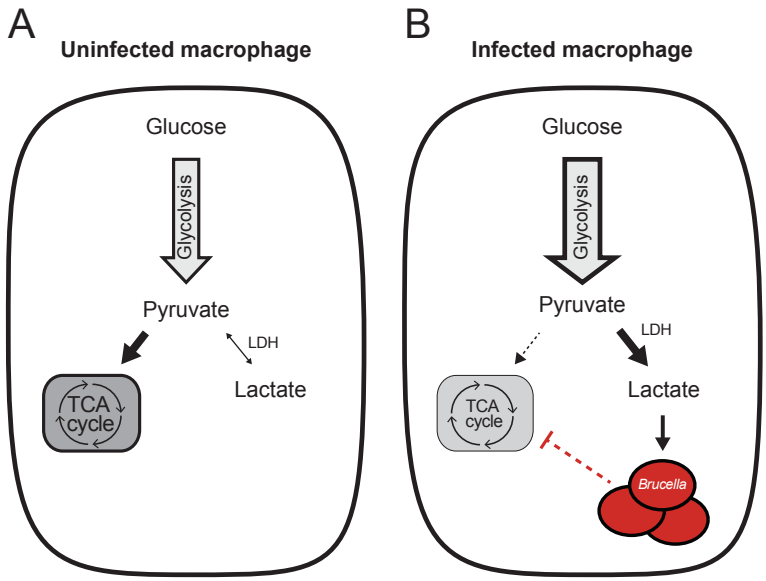

FIG 7. Model of how *B. abortus* exploits the shift to Warburg-like metabolism in macrophages.

Data presented in this study support a model in which inhibition of tricarboxylic acid (TCA) cycle metabolism upon infection biases the host cell toward the production of lactic acid. **(A)** Uninfected macrophages exhibit typical central carbon metabolism in which pyruvate enters the TCA cycle. **(B)** *B. abortus* infection biases the macrophage toward aerobic glycolysis and lactate production. *B. abortus* efficiently utilizes lactic acid via the lactate dehydrogenase (LDH) enzyme, LldD. A strain lacking *lldD* is compromised in axenic lactic acid metabolism and in intracellular replication in a THP-1 macrophage model. Pharmacological inhibition of host glycolysis or LDH-A inhibits *B. abortus* replication.